^{18}F-FDG PET Dissemination Features in Diffuse Large B-Cell Lymphoma Are Predictive of Outcome

Anne-Ségolène Cottereau[1,2], Christophe Nioche[2], Anne-Sophie Dirand[2], Jérôme Clerc[1], Franck Morschhauser[3], Olivier Casasnovas[4], Michel Meignan[5], and Irène Buvat[2]

[1]Department of Nuclear Medicine, Cochin Hospital, Assistance Publique Hôpitaux de Paris and Paris Descartes University, Paris, France; [2]Imagerie Moléculaire In Vivo, CEA, INSERM, Université Paris Sud, CNRS, Université Paris Saclay, Orsay, France; [3]Groupe de Recherche sur les formes Injectables et les Technologies Associées, Université Lille, CHU Lille, Lille, France; [4]Hematology Department, Dijon Hospital, and INSERM 1231, Bourgogne Franche Comte University, Dijon, France; and [5]LYSA Imaging, Creteil, France

We assessed the predictive value of new radiomic features characterizing lesion dissemination in baseline ^{18}F-FDG PET and tested whether combining them with baseline metabolic tumor volume (MTV) could improve prediction of progression-free survival (PFS) and overall survival (OS) in diffuse large B-cell lymphoma (DLBCL) patients. **Methods:** From the LNH073B trial (NCT00498043), patients with advanced-stage DLCBL and ^{18}F-FDG PET/CT images available for review were selected. MTV and several radiomic features, including the distance between the 2 lesions that were farthest apart ($Dmax_{patient}$), were calculated. Receiver-operating-characteristic analysis was used to determine the optimal cutoff for quantitative variables, and Kaplan–Meier survival analyses were performed. **Results:** With a median age of 46 y, 95 patients were enrolled, half of them treated with R-CHOP biweekly (rituximab, cyclophosphamide, doxorubicin, vincristine, and prednisone) and the other half with R-ACVBP (rituximab, doxorubicin, cyclophosphamide, vindesine, bleomycin, and prednisone), with no significant impact on outcome. Median MTV and $Dmax_{patient}$ were 375 cm^3 and 45 cm, respectively. The median follow-up was 44 mo. High MTV and $Dmax_{patient}$ were adverse factors for PFS ($P = 0.027$ and $P = 0.0003$, respectively) and for OS ($P = 0.0007$ and $P = 0.0095$, respectively). In multivariate analysis, only $Dmax_{patient}$ was significantly associated with PFS ($P = 0.0014$) whereas both factors remained significant for OS ($P = 0.037$ and $P = 0.0029$, respectively). Combining MTV (>384 cm^3) and $Dmax_{patient}$ (>58 cm) yielded 3 risk groups for PFS ($P = 0.0003$) and OS ($P = 0.0011$): high with 2 adverse factors (4-y PFS and OS of 50% and 53%, respectively, $n = 18$), low with no adverse factor (94% and 97%, $n = 36$), and an intermediate category with 1 adverse factor (73% and 88%, $n = 41$). **Conclusion:** Combining MTV with a parameter reflecting the tumor burden dissemination further improves DLBCL patient risk stratification at staging.

Key Words: oncology; lymphoma; ^{18}F-FDG PET/CT; DLBCL; dissemination; metabolic tumor volume

J Nucl Med 2020; 61:40–45
DOI: 10.2967/jnumed.119.229450

Diffuse large B-cell lymphoma (DLBCL) represents the most frequent types of lymphoid cancer, accounting for approximately 25% of non-Hodgkin lymphoma (*1*). The current first-line treatment, R-CHOP (rituximab, a CD-20-directed monoclonal antibody, given in combination with the standard chemotherapeutic regimen of cyclophosphamide, doxorubicin, vincristine, and prednisone), is effective in 60%–70% of patients (*2*). For the 30%–40% of patients who will exhibit refractory disease or relapse after initial response, the prognosis is poor. The life expectancy for patients with refractory disease or early relapse is dramatically reduced because salvage regimens lead to very modest response rates (*3,4*). A personalized approach toward first-line treatment might improve DLBCL patients' outcome. Interim PET performed after 2 or 4 cycles of chemotherapy has been proposed as a tool for tailoring therapy, but no therapeutic approach has proven successful to improve the prognosis of interim PET–positive patients. An earlier risk stratification is therefore still needed. High-risk patients are not accurately identified by the current prognostic scoring systems, such as the International Prognostic Index (IPI) (*5*), the revised IPI (*6*), or the National Comprehensive Cancer Network IPI (*7*). Over the last 5 y, the prognostic role of quantitative PET parameters, in particular the metabolic tumor volume (MTV), has been demonstrated in many lymphoma subtypes (*8,9*), including DLBCL (*10–12*). MTV reflects the total volume of ^{18}F-FDG–avid tumor regions within the whole body and hence provides a more comprehensive tumor burden evaluation than previous surrogates such as lactate dehydrogenase levels. Patients with a high tumor burden are at higher risk for treatment failure and shorter survival than those with a low tumor burden. However, this parameter does not account for the spatial distribution of the lesions throughout the body. Yet chemokine receptor 4 (CXCR4) expression has been shown to be a marker of bad prognosis in DLBCL (*13,14*). Because CXCR4 expression mediates dissemination of DLBCL cells, our assumption was that the prognostic value of MTV might be improved by combining the tumor burden estimate with a quantitative feature reflecting spread of the disease. The aim of this study was to define and analyze new ^{18}F-FDG PET metrics describing tumor dissemination and to determine their added predictive value to MTV for DLBCL patients included in the LNH073B trial (*15*).

MATERIALS AND METHODS

Patients

Details and results of the LNH073B study design (the study was registered at ClinicalTrials.gov: NCT00498043) have been published

Received Apr. 8, 2019; revision accepted Jun. 3, 2019.
For correspondence or reprints contact: Anne-Ségolène Cottereau, Nuclear Medicine Department, Cochin Hospital, Assistance Publique Hôpitaux de Paris, Paris Descartes University, 75014 Paris, France.
E-mail: annesegolene.cottereau@aphp.fr
Published online Jun. 14, 2019.

elsewhere (*15*). In brief, DLBCL patients with an age-adjusted IPI score of 2 or 3 were randomly assigned to induction immunochemotherapy with 4 cycles of either R-CHOP biweekly or R-ACVBP (rituximab, doxorubicin, cyclophosphamide, vindesine, bleomycin, and prednisone). Consolidation treatment was driven by centrally reviewed PET assessment according to visual criteria after 2 and 4 treatment cycles. A baseline PET scan was mandatory, with at least 1 evaluable hypermetabolic lesion. Ethics approval was obtained for this trial, and all patients provided written informed consent to participate.

For the current analysis, only Ann Arbor stage 3 and 4 patients whose MTV could be computed from a baseline PET/CT scan and with at least 2 detectable lesions allowing distance measurement were included.

Baseline patient and disease characteristics, including individual components of the age-adjusted IPI score, progression-free survival (PFS), and overall survival (OS) defined according to the revised National Cancer Institute criteria, were obtained (*16*).

PET/CT Scanning and Quantitative Analysis

Baseline PET image data in anonymized DICOM format were collected for functional parameter measurements. Quality control rejected scans with burning errors in DICOM retrieval or with a delay of more than 90 min between ^{18}F-FDG injection and scanning.

The PET data were analyzed by a nuclear medicine physician masked to patient outcome, using LIFEx software (*17*). Calculation of MTV was based on a supervised segmentation of tumor regions involving 41% SUV_{max} thresholding of automatically detected hypermetabolic regions. MTV was defined as the sum of the metabolic volumes of every individual lesion. For each lesion, tumor lesion glycolysis was calculated as the product of the lesion volume by the SUV_{mean} within the lesion, and total lesion glycolysis was obtained by summing tumor lesion glycolysis over all lesions. The highest SUV_{max} of the patient over all lesions and the number of lesions were also reported. Last, several features reflecting the spatial distributions of malignant foci throughout the whole body were computed, based on distance measurements between lesions. Each lesion location was defined as the position of its center, and the distances between 2 lesions were calculated using the Euclidian distance between their centers.

Four dissemination features were calculated in LIFEx: the distance between the 2 lesions that were farthest apart ($Dmax_{patient}$), the distance between the largest lesion and the lesion farthest from that bulk ($Dmax_{bulk}$), the sum of the distances of the bulky lesion from all other lesions ($SPREAD_{bulk}$), and the largest value, over all lesions, of the sum of the distances from a lesion to all the others ($SPREAD_{patient}$).

MTV was also calculated with FIJI software by an independent nuclear physician, based on the same 41% SUV_{max} threshold method. The reproducibility of MTV measurements between LIFEx and FIJI software was assessed.

Statistical Analysis

For each PET-derived feature, receiver-operating-characteristic (ROC) analysis was used to define the optimal cutoff for predicting the occurrence of an event (PFS or OS) by maximizing the Youden index (sensitivity + specificity − 1). Sensitivity and specificity were calculated for that cutoff. Only features with an area under the ROC curve (AUC) greater than 0.6 on PFS were retained for subsequent analyses. Survival functions were calculated using Kaplan–Meier analyses, and the survival distributions were compared using the log-rank test. Multivariate analyses involving MTV and dissemination features were performed using Cox proportional hazards models. On the basis of these results, a prognostic model combining MTV and a dissemination feature was built on which Kaplan–Meier survival analysis was performed. Correlations between dissemination features and MTV were assessed using χ^2 tests. Mann–Whitney tests were used to determine whether patient size and MTV significantly differed in patients with low and high dissemination features. The reproducibility of MTV measurement between the 2 operators and the 2 types of software was assessed by the Lin concordance correlation coefficient, and interobserver agreement was assessed using κ-statistics.

Statistical significance was set at a P value of less than 0.05. All statistical analyses were performed using MedCalc software.

TABLE 1
Patient Characteristics (n = 95)

Characteristic	Data
Sex	
F	42 (44%)
M	53 (56%)
Age (y)	46 (18–59)
Height (cm)	173 (140–193)
≤170 cm	42 (44.2%)
>170 cm	53 (55.8%)
Ann Arbor stage	
III	9 (9.5%)
IV	86 (90.5%)
Performance status	
1	27 (28.4%)
2	44 (46.3%)
3	19 (20%)
4	5 (5.3%)
Age-adjusted IPI	
1	3 (3%)
2	69 (73%)
3	23 (24%)
Treatment	
R-ACVBP biweekly	46 (48%)
R-CHOP biweekly	49 (52%)

Qualitative data are expressed as numbers followed by percentages in parentheses; continuous data are expressed as median followed by range in parentheses.

TABLE 2
Median, Range, Mean, and SD of PET Features

Parameter	Median	Range	Mean	SD
MTV (cm^3)	375	27–2,525	469	392
SUV_{max}	20	4–49	21	8
Total lesion glycolysis	3,275	166–19,428	4,298	3,323
$Dmax_{patient}$ (cm)	45	7–135	46	25
$Dmax_{Bulk}$ (cm)	32	7–101	32	17.5
$SPREAD_{patient}$ (cm)	367	7–11,915	798	1,420
$SPREAD_{bulk}$ (cm)	205	7–4,561	425.4	620
VOIs per patient (n)	13	2–130	20	21

TABLE 3
ROC Analysis of PET Features, AUC, Sensitivity, and Specificity

Parameter	PFS				OS			
	AUC	Cutoff	Se	Sp	AUC	Cutoff	Se	Sp
MTV (cm^3)	0.64	394	68	60	0.69	468	77	71
SUV_{max}	0.58	15	41	85	0.53	23	46	71
Total lesion glycolysis	0.53	4,396	45	68	0.67	4,550	61	73
$Dmax_{patient}$ (cm)	0.65	58	68	74	0.59	58	69	69
$Dmax_{bulk}$ (cm)	0.63	43	54	82	0.60	43	54	80
$SPREAD_{patient}$ (cm)	0.65	1,023	50	85	0.58	716	54	71
$SPREAD_{bulk}$ (cm)	0.65	530	54	86	0.59	407	61	71
VOIs per patient (*n*)	0.64	23	54	77	0.57	20	54	67

Se = sensitivity; Sp = specificity.

RESULTS

In total, 95 patients were included, whose clinical characteristics are summarized in Table 1.

With a median follow-up of 44 mo (range, 27–63 mo), the 4-y PFS and OS rates for the whole group were 77% and 85%, respectively. Twenty-two patients had a PFS event, with a median of 7 mo: 12 in the R-CHOP group and 10 in the R-ACVBP group. Thirteen patients died, at a median of 13 mo: 8 in the R-CHOP group and 5 in the R-ACVBP group. Using log rank tests, neither performance status (0–1 vs. 2–3) nor age-adjusted IPI (2 vs. 3) was significantly associated with PFS ($P = 0.17$ and $P = 0.21$, respectively) or OS ($P = 0.41$ and $P = 0.46$, respectively). The chemotherapy regimen (R-CHOP vs. R-ACVBP) had no significant prognostic impact on either PFS ($P = 0.69$) or OS ($P = 0.48$).

PET Features

Table 2 shows the descriptive statistics for the PET features, and Table 3 gives the results of the ROC analyses performed on each PET parameter.

Using an ROC optimal cutoff, MTV was highly predictive of outcome (PFS: $P = 0.027$; OS: $P = 0.0007$) (Table 4). Patients with a high MTV had a significantly worse outcome, with a 4-y PFS and OS of 67% and 73%, versus 84% and 95% for patients with a lower MTV (Fig. 1).

MTV calculation with 2 different software programs was reproducible, with a Lin concordance correlation coefficient of 0.85 (0.79–0.89) and a κ of 0.86, suggesting overall good agreement.

Regarding the dissemination features, ROC AUCs were always greater than 0.6 for PFS and close to 0.6 for OS (Table 3). Table 4 shows that a $Dmax_{patient}$ of more than 58 cm, a $Dmax_{bulk}$ of more than 43 cm, a $SPREAD_{patient}$ of more than 1,020 cm, and a $SPREAD_{bulk}$ of more than 530 cm were negative prognostic factors for PFS ($P = 0.0003$, $P = 0.0003$, $P = 0.0011$, and $P < 0.0001$, respectively) and that for OS, only $Dmax_{patient}$ and $Dmax_{bulk}$ were statistically significant ($P = 0.0095$ and $P = 0.023$, respectively; Fig. 2).

No significant differences in height were observed between patients with low and high $Dmax_{patient}$ ($P = 0.96$). Similarly, no significant differences in MTV were observed between patients with low and high $Dmax_{patient}$ (median of 344 cm^3 and 415 cm^3, respectively, $P = 0.14$).

Combination of MTV and Dissemination Features

In multivariate Cox regression analysis including MTV and $Dmax_{patient}$, $Dmax_{patient}$ was significantly associated with PFS ($P = 0.0014$; hazard ratio, 4.3) whereas MTV was not ($P = 0.056$; hazard ratio, 2.3). For OS, both MTV ($P = 0.037$; hazard ratio, 4.0) and $Dmax_{patient}$ ($P = 0.029$; hazard ratio, 3.7) were significant.

Three risk categories could therefore be significantly distinguished on the basis of the presence or absence of high MTV (>394 cm^3) or $Dmax_{patient}$ (>58 cm) ($P = 0.0003$ for PFS and

TABLE 4
PET Parameters Associated with PFS and OS in Log-Rank Cox Tests

Parameter	PFS			OS		
	HR	4-y PFS	*P*	HR	4-y OS	*P*
Low MTV	1 (ref)	84% (79–89)	0.027	1 (ref)	95% (92–98)	0.0007
High MTV	2.6 (1.1–6.0)	67% (60–74)		6.9 (2.1–21.9)	66% (56–76)	
Low $Dmax_{patient}$	1 (ref)	88% (84–92)	0.0003	1 (ref)	93% (90–96)	0.0095
High $Dmax_{patient}$	4.6 (1.9–11.2)	55% (47–63)		4.2 (1.3–13.1)	69% (60–78)	
Low $Dmax_{bulk}$	1 (ref)	86% (82–90)	0.0003	1 (ref)	91% (88–94)	0.023
High $Dmax_{bulk}$	4.1 (1.5–11.3)	52% (42–62)		3.3 (1–11.3)	68% (57–79)	
Low $SPREAD_{patient}$	1 (ref)	85% (81–89)	0.0011	1 (ref)	86% (81–91)	0.24
High $SPREAD_{patient}$	3.7 (1.3–10,1)	52% (42–62)		1.9 (0.5–6.8)	78% (70–85)	
Low $SPREAD_{bulk}$	1	86% (82–90)	<0.0001	1 (ref)	90% (87–93)	0.056
High $SPREAD_{bulk}$	4.9 (1.7–13.9)	45% (35–55)		2.8 (0.8–9.9)	69% (59–79)	
Low no. of ROIs	1 (ref)	85% (81–89)	0.0052	1 (ref)	87% (82–92)	0.21
High no. of ROIs	3.1 (1.2–7.9)	58% (49–67)		1.9 (0.6–6.4)	79% (72–86)	

HR = hazard ratio.
Data in parentheses are 95% confidence intervals.

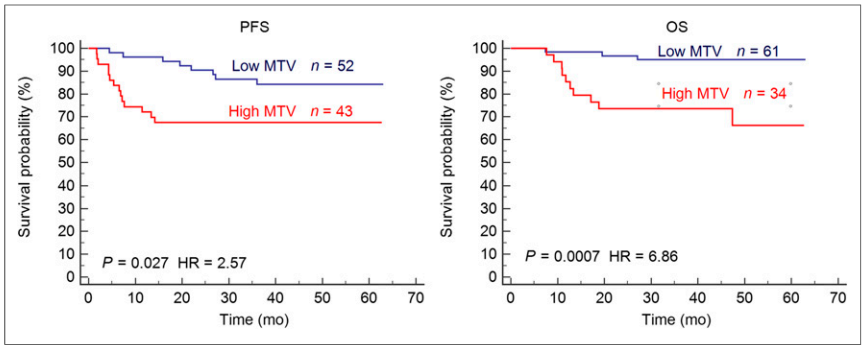

FIGURE 1. Kaplan–Meier estimates of PFS and OS according to MTV. HR = hazard ratio.

$P = 0.0011$ for OS) (Fig. 3): group 1 with no risk factor ($n = 36$), group 2 with 1 risk factor only ($n = 41$), and group 3 with both ($n = 18$), with 4-y PFS rates of 94%, 73%, and 50%, respectively, and 4-y OS rates of 97%, 88%, and 53%, respectively. Group 2 versus group 3 had significantly different PFS ($P = 0.041$) and OS ($P = 0.019$); group 1 versus group 2 had significantly different PFS ($P = 0.013$) whereas OS did not reach significance ($P = 0.13$). Figure 4 shows examples of ^{18}F-FDG PET images (maximum-intensity projections) of patients from groups 2 and 3.

DISCUSSION

Lymphoma is a group of blood cancers that develop from lymphocytes. Although most cells in the body can migrate at one or more distinct steps during their development and differentiation, the trafficking propensity of lymphocytes is unrivaled among somatic cells. In cases of malignant transformation, this property allows for rapid tumor dissemination irrespective of the conventional anatomic boundaries limiting early spread in most types of cancer. Thus, the disease can spread rapidly to different parts of the body, involving lymph nodes, possibly associated with extranodal sites (*18*).

^{18}F-FDG PET/CT is the current state-of-the-art imaging scan in lymphoma. Recent advances in PET imaging revealed that MTV, as a surrogate for tumor cell number, has a strong prognostic value in DLBCL, much higher than the presence of bulk (*10,11*). Recently, this prognostic value was confirmed in a large phase 3 study, GOYA, including more than 1,100 patients (NCT01287741 (*19*)): MTV quartiles stratified the population in quartiles 1, 2, 3, and 4 with a 3-y PFS of 86%, 84%, 78%, and 66%, respectively (*20*). In the present study, we demonstrated that MTV maintained its prognostic power in a cohort of patients with advanced-stage disease. Patients with stage 3 or 4 were significantly stratified in 2 different risk categories according to their MTV. Moreover, using ROC analysis, MTV was the only significant feature in both PFS and OS. It was superior to standard features such as age-adjusted IPI for both PFS and OS. A high MTV identified 64% of the PFS events (14/22).

In this study, we introduced new radiomic features extracted from PET scans to quantify tumor dissemination. Several of these features based on distance measurement between lymphoma lesions were significant for PFS and OS in our group of stage 3 and stage 4 patients, suggesting that an advanced characterization of lesion dissemination is relevant even among patients with advanced disease. In particular, $Dmax_{patient}$ had strong predictive power for PFS and OS. A high $Dmax_{patient}$ was associated with an adverse outcome, with a 4-y PFS and OS of 55% and 69%, respectively. Similarly, $SPREAD_{patient}$ and $SPREAD_{bulk}$ combining spatial spread information and the number of lesions were very significantly associated with PFS (Table 4).

$Dmax_{patient}$ is a 3-dimensional feature simple to calculate, with an intuitive interpretation. Height did not influence $Dmax_{patient}$, as height did not significantly differ between high- and low-$Dmax_{patient}$ groups. Given that the distance between 2 lesions is calculated on the basis of their respective centers, the $Dmax_{patient}$ is not highly dependent on the lesion contours and on the fact that the contours are rather loose or tight depending on the delineation tool settings that are used. This is an asset to ensure good reproducibility.

Combining MTV and $Dmax_{patient}$ made it possible to identify a group with a poor prognosis so that clinicians might consider changing treatment. Indeed, patients with high baseline MTV (>394 cm^3) and high $Dmax_{patient}$ (>58 cm) had a much worse prognosis than the other patients, with 4-y PFS of 50% and 4-y OS of 53%. This group represented 19% of the cohort and included 41% of the PFS total number of events (9/22) and 54% of the OS total number of events, making this model useful for identifying patients with a poor prognosis.

In the LNH073B trial, consolidation treatment was driven by centrally reviewed PET assessment after 2 (denoted PET 2) and 4 (denoted PET 4) cycles: patients who were classified as PET 2– and PET 4–negative received standard immunochemotherapy consolidation; patients classified as PET 2–positive and PET 4–negative received 2 cycles of high-dose methotrexate (3 g/m^2) and then a high-dose therapy (carmustine, etoposide, cytarabine, and melphalan [BEAM] or Zevalin [ibritumomab tiuxetan; Acrotech biopharma] and BEAM [Z-BEAM]), followed by autologous stem cell transplantation; PET 4–positive patients had a salvage regimen followed by autologous stem cell transplantation in responders to salvage. Despite this ^{18}F-FDG PET–driven consolidation strategy that might actually decrease the prognostic impact of baseline PET features, MTV and dissemination features remained significantly predictive of PFS and OS. Further studies are needed to more comprehensively establish the role dissemination features might play in

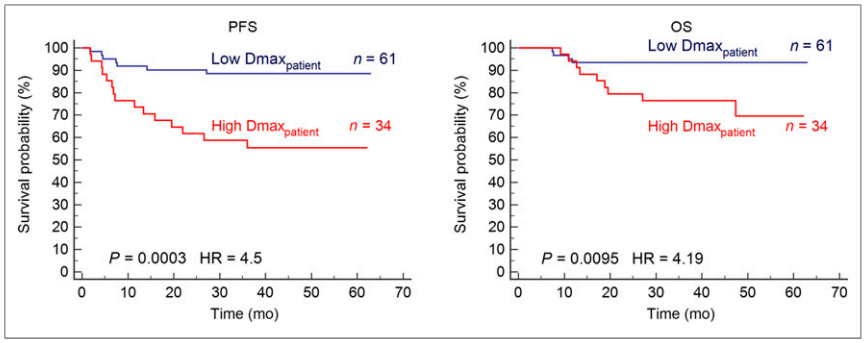

FIGURE 2. Kaplan–Meier estimates of PFS and OS according to $Dmax_{patient}$. HR = hazard ratio.

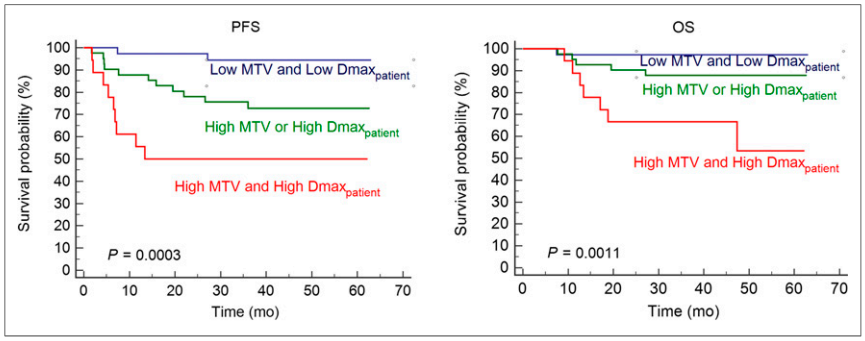

FIGURE 3. Kaplan–Meier estimates of PFS and OS according to baseline MTV and Dmax$_{patient}$.

lymphomas when measured at baseline and during patient monitoring. Indeed, it has been shown that dysregulated CXCR4 expression predicts disease progression in DLBCL and that CXCR4 overexpression impairs rituximab response and the prognosis of R-CHOP–treated DLBCL patients (*21*). In addition, MTV influences the rituximab pharmacokinetics (*22*). Patients with a high MTV had a lower AUC of rituximab concentration, and low AUCs are associated with lower response rate, shorter PFS, and shorter OS. The observed prognostic value of the dissemination biomarker we propose is consistent with the association between CXCR4 overexpression and rituximab resistance. The relationship between CXCR4 expression and radiomic features reflecting the spread of the disease would be worth investigating to determine whether radiomic features can actually partly reflect CXCR4 expression. Imaging of CXCR4 could also be helpful in this regard (*23*).

There are many molecular and imaging biomarkers proposed for baseline prognostic prediction in DLBCL, among which the most recent circulating tumor DNA has been correlated with TMTV and PET response after treatment (*24*). The respective role of these new imaging and molecular biomarkers will have to be determined in large prospective studies for personalized therapeutic approaches.

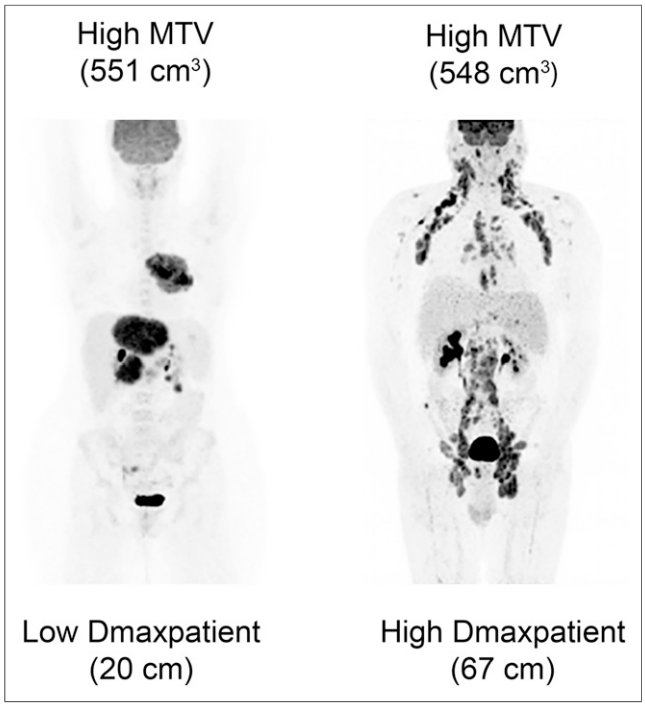

FIGURE 4. (Left) Example patient with high MTV and low Dmax$_{patient}$ (group 2). (Right) Example patient with both high MTV and high Dmax$_{patient}$ (group 3).

CONCLUSION

^{18}F-FDG PET/CT can provide a predictive radiomic signature combining metrics reflecting tumor dissemination and tumor burden. In this study of advanced-stage DLBCL patients, combining MTV and Dmax$_{patient}$ improved patient risk stratification at staging.

DISCLOSURE

No potential conflict of interest relevant to this article was reported.

KEY POINTS

QUESTION: Could new radiomic features characterizing lesion dissemination in baseline ^{18}F-FDG PET improve survival prediction in DLBCL patients?

PERTINENT FINDINGS: In a cohort of 95 DLBCL patients from the LNH073B trial, new radiomic features extracted from PET scans based on distance measurement between lymphoma lesions were significant for PFS and OS prediction. Combining MTV with a parameter reflecting tumor burden dissemination further improves DLBCL patient risk stratification at staging.

IMPLICATIONS FOR PATIENT CARE: Combining metrics reflecting tumor dissemination with MTV identified a group of high-risk patients who might benefit from new therapeutic strategies.

REFERENCES

1. Teras LR, DeSantis CE, Cerhan JR, Morton LM, Jemal A, Flowers CR. 2016 US lymphoid malignancy statistics by World Health Organization subtypes. *CA Cancer J Clin.* 2016;66:443–459.
2. Tilly H, Gomes da Silva M, Vitolo U, et al. Diffuse large B-cell lymphoma (DLBCL): ESMO clinical practice guidelines for diagnosis, treatment and follow-up. *Ann Oncol.* 2015;26(suppl 5):v116–v125.
3. Gisselbrecht C, Glass B, Mounier N, et al. Salvage regimens with autologous transplantation for relapsed large B-cell lymphoma in the rituximab era. *J Clin Oncol.* 2010;28:4184–4190.
4. Crump M, Neelapu SS, Farooq U, et al. Outcomes in refractory diffuse large B-cell lymphoma: results from the international SCHOLAR-1 study. *Blood.* 2017;130:1800–1808.
5. International Non-Hodgkin's Lymphoma Prognostic Factors Project. A predictive model for aggressive non-Hodgkin's lymphoma. *N Engl J Med.* 1993;329:987–994.
6. Sehn LH, Berry B, Chhanabhai M, et al. The revised International Prognostic Index (R-IPI) is a better predictor of outcome than the standard IPI for patients with diffuse large B-cell lymphoma treated with R-CHOP. *Blood.* 2007;109:1857–1861.
7. Zhou Z, Sehn LH, Rademaker AW, et al. An enhanced International Prognostic Index (NCCN-IPI) for patients with diffuse large B-cell lymphoma treated in the rituximab era. *Blood.* 2014;123:837–842.
8. Meignan M, Cottereau AS, Versari A, et al. Baseline metabolic tumor volume predicts outcome in high-tumor-burden follicular lymphoma: a pooled analysis of three multicenter studies. *J Clin Oncol.* 2016;34:3618–3626.
9. Casasnova RO, Kanoun S, Tal I, Cottereau AS, et al. Baseline total metabolic volume (TMTV) to predict the outcome of patients with advanced Hodgkin lymphoma (HL) enrolled in the AHL2011 LYSA trial [abstract]. *J Clin Oncol.* 2016;34(suppl):7509.

10. Mikhaeel NG, Smith D, Dunn JT, et al. Combination of baseline metabolic tumour volume and early response on PET/CT improves progression-free survival prediction in DLBCL. *Eur J Nucl Med Mol Imaging.* 2016;43:1209–1219.
11. Cottereau AS, Lanic H, Mareschal S, et al. Molecular profile and FDG-PET/CT total metabolic tumor volume improve risk classification at diagnosis for patients with diffuse large B-cell lymphoma. *Clin Cancer Res.* 2016;22:3801–3809.
12. Toledano MN, Desbordes P, Banjar A, et al. Combination of baseline FDG PET/CT total metabolic tumour volume and gene expression profile have a robust predictive value in patients with diffuse large B-cell lymphoma. *Eur J Nucl Med Mol Imaging.* 2018;45:680–688.
13. Moreno MJ, Bosch R, Dieguez-Gonzalez R, et al. CXCR4 expression enhances diffuse large B cell lymphoma dissemination and decreases patient survival. *J Pathol.* 2015;235:445–455.
14. Chen J, Xu-Monette ZY, Deng L, et al. Dysregulated CXCR4 expression promotes lymphoma cell survival and independently predicts disease progression in germinal center B-cell-like diffuse large B-cell lymphoma. *Oncotarget.* 2015;6:5597–5614.
15. Casasnovas RO, Ysebaert L, Thieblemont C, et al. FDG-PET-driven consolidation strategy in diffuse large B-cell lymphoma: final results of a randomized phase 2 study. *Blood.* 2017;130:1315–1326.
16. Cheson BD, Pfistner B, Juweid ME, et al. Revised response criteria for malignant lymphoma. *J Clin Oncol.* 2007;25:579–586.
17. Nioche C, Orlhac F, Boughdad S, et al. LIFEx: a freeware for radiomic feature calculation in multimodality imaging to accelerate advances in the characterization of tumor heterogeneity. *Cancer Res.* 2018;78:4786–4789.
18. Pals ST, de Gorter DJ, Spaargaren M. Lymphoma dissemination: the other face of lymphocyte homing. *Blood.* 2007;110:3102–3111.
19. Vitolo U, Trneny M, Belada D, et al. Obinutuzumab or rituximab plus cyclophosphamide, doxorubicin, vincristine, and prednisone in previously untreated diffuse large B-cell lymphoma. *J Clin Oncol.* 2017;35:3529–3537.
20. Kostakoglu L, Martelli M, Sehn LH, et al. Baseline PET-derived metabolic tumor volume metrics predict progression-free and overall survival in DLBCL after first-line treatment: results from the phase 3 GOYA study [abstract]. *Blood.* 2017;130(suppl):824.
21. Laursen MB, Reinholdt L, Schönherz AA, et al. High CXCR4 expression impairs rituximab response and the prognosis of R-CHOP-treated diffuse large B-cell lymphoma patients. *Oncotarget.* 2019;10:717–731.
22. Tout M, Casasnovas O, Meignan M, et al. High CXCR4 expression impairs rituximab response and the prognosis of R-CHOP-treated diffuse large B-cell lymphoma patients. *Blood.* 2017;129:2616–2623.
23. Wester HJ, Keller U, Schottelius M, et al. Disclosing the CXCR4 expression in lymphoproliferative diseases by targeted molecular imaging. *Theranostics.* 2015;5:618–630.
24. Kurtz DM, Scherer F, Jin MC, et al. Circulating tumor DNA measurements as early outcome predictors in diffuse large B-cell lymphoma. *J Clin Oncol.* 2018;36:2845–2853.